

Article

Magneto-Thermoelastic Response in an Unbounded Medium Containing a Spherical Hole via Multi-Time-Derivative Thermoelasticity Theories

Ashraf M. Zenkour ^{1,2,*} , Daoud S. Mashat ¹ and Ashraf M. Allehaibi ^{1,3} 

¹ Department of Mathematics, Faculty of Science, King Abdulaziz University, P.O. Box 80203, Jeddah 21589, Saudi Arabia; dmashat@kau.edu.sa (D.S.M.); amlehaibi@uqu.edu.sa (A.M.A.)

² Department of Mathematics, Faculty of Science, Kafrelsheikh University, Kafrelsheikh 33516, Egypt

³ Department of Mathematics, Jamoum University College, Umm Al-Qura University, Jamoum, Makkah 21955, Saudi Arabia

* Correspondence: zenkour@kau.edu.sa or zenkour@sci.kfs.edu.eg

Abstract: This article introduces magneto-thermoelastic exchanges in an unbounded medium with a spherical cavity. A refined multi-time-derivative dual-phase-lag thermoelasticity model is applied for this reason. The surface of the spherical hole is considered traction-free and under both constant heating and external magnetic field. A generalized magneto-thermoelastic coupled solution is developed utilizing Laplace's transform. The field variables are shown graphically and examined to demonstrate the impacts of the magnetic field, phase-lags, and other parameters on the field quantities. The present theory is examined to assess its validity including comparison with the existing literature.

Keywords: CTE, L–S, and G–N models; spherical hole; multi-phase-lag



Citation: Zenkour, A.M.; Mashat, D.S.; Allehaibi, A.M. Magneto-Thermoelastic Response in an Unbounded Medium Containing a Spherical Hole via Multi-Time-Derivative Thermoelasticity Theories. *Materials* **2022**, *15*, 2432. <https://doi.org/10.3390/ma15072432>

Academic Editors: Stelios K. Georgantzinis, Georgios I. Giannopoulos, Konstantinos Stamoulis and Stylianos Markolefas

Received: 13 January 2022

Accepted: 21 March 2022

Published: 25 March 2022

Publisher's Note: MDPI stays neutral with regard to jurisdictional claims in published maps and institutional affiliations.



Copyright: © 2022 by the authors. Licensee MDPI, Basel, Switzerland. This article is an open access article distributed under the terms and conditions of the Creative Commons Attribution (CC BY) license (<https://creativecommons.org/licenses/by/4.0/>).

1. Introduction

The thermoelastic responses of different structures with spherical cavities have received much attention because of their usefulness in many industrial applications. In the following, we restrict our attention to the application of continua with spherical cavities. All the problems discussed are concerned with thermoelastic exchanges within the framework of several generalized thermoelasticity theories.

Generalized thermoelasticity models, with one or more relaxation times, have been proposed to modify the heat conduction equation. One of the original forms of the heat conduction equation, associated with gases theory, was introduced by Maxwell [1]. Another form was proposed within the framework of heat conduction in rigid structures by Cattaneo [2]. A third form was introduced by Dhaliwal and Sherief [3] by extension to the case of an anisotropic medium. To overcome the contradiction of an endless velocity of thermal waves intrinsic to classical coupled thermoelasticity (CTE) theory [4], attempts have been made by various investigators, for a range of reasons, to modify coupled thermoelasticity to entail a wave-type heat conduction equation.

Lord and Shulman (L–S) [5] developed generalized thermoelasticity theory presenting one relaxation time in Fourier's law of heat conduction equation and therefore converting it into a hyperbolic type. Banerjee and Roychoudhuri [6] discussed the generalized theory of thermo-elasticity suggested by L–S [5] to examine thermo-visco-elastic wave propagation in an unlimited viscoelastic body of Kelvin–Voight type with a spherical hole. Sinha and Elsibai [7] discussed thermoelastic exchanges in an unlimited solid with a spherical inclusion considering L–S and G–L theories. Rakshit Kundu and Mukhopadhyay [8] described field variables in a viscoelastic body with a spherical hole. Youssef [9] described a problem of thermoelastic exchanges in a limitless body including a spherical hole subjected

to a moving heat source according to L–S theory. Elhagary [10] described the problem of a thermoelastic unbounded solid including a spherical hole in the framework of L–S diffusion theory. Karmakar et al. [11] determined the temperatures, stress, displacement, and strain in an unbounded solid including a spherical hole in the framework of processes addressed by two-temperature theory (2TT).

Later, Green–Naghdi (G–N) [12–14] created three versions for generalized thermoelasticity that were identified as I, II, and III types. Mukhopadhyay [15,16] presented thermoelastic exchanges in an unbounded solid including a spherical hole in the framework of G–N theory. Mukhopadhyay and Kumar [17] considered thermoelastic exchanges in an infinite solid with a spherical hole in the framework of several theories. Allam et al. [18] investigated electro-magneto-thermoelastic exchanges in an infinite solid with a spherical hole in the framework of G–N theory. Banik and Kanoria [19] determined the thermoelastic quantities in an infinite solid with a spherical inclusion in the framework of the 2TT. Abbas [20] investigated a general solution to the field equations of 2TT in an unbounded medium with a spherical hole in the framework of the G–N model. Bera et al. [21] investigated the waves arising from the boundary of a spherical cavity in an infinite medium. Biswas [22] examined the thermoelastic exchange in a limitless body including a spherical cavity in the context of the G–N model. Chandrasekharaiah and Narasimha Murthy [23] considered thermoelastic exchanges in an infinite body including a spherical inclusion.

Green and Lindsay [24] pioneered an additional theory, known as the G–L model, that included two relaxation times. Roy Choudhuri and Chatterjee [25] studied spherically symmetric thermoelastic waves in an unbounded body containing a spherical hole. Sherief and Darwish [26] presented a problem of a thermoelastic unbounded solid containing a spherical hole in the framework of thermoelasticity theory with two relaxation times. Mukhopadhyay [27] discussed thermally induced vibrations of an unbounded viscoelastic body including a spherical hole in the framework of G–L theory. Ghosh and Kanoria [28] determined thermoelastic quantities in a functionally graded (FG) spherically unbounded body including a spherical hole in the framework of G–L theory. Kanoria and Ghosh [29] examined thermoelastic exchanges in an FG hollow sphere in the framework of the G–L model. Das and Lahiri [30] considered a thermoelastic problem for an unbounded FG and temperature-dependent spherical inclusion in the framework of G–L theory.

Many investigators have used dual/triple-phase-lag (D/TPL) heat transfer theory to examine thermoelastic exchanges in unbounded mediums including spherical cavities. DPL theory was originally presented by Tzou [31,32] to describe some problems at a macroscopic scale. Abouelregal and Abo-Dahab [33] presented thermal quantities in an unbounded solid with a spherical hole in the framework of DPL theory. Hobiny and Abbas [34] applied DPL theory in the examination of photo-thermal exchanges in an infinite solid containing a spherical cavity. Mondal and Sur [35] studied a coupled problem in an infinite solid with a spherical hole in the framework of a photothermal transport process in relation to 2TT. Singh and Sarkar [36] examined thermoelastic exchange in a 2TT unbounded isotropic body containing a spherical cavity in the framework of a memory-dependent derivative (MDD). Comparisons were made graphically between the 2T TPL theory and 2T L–S theory with MDD. Many researchers have dealt with one-dimensional (1D) problems in generalized thermoelasticity in unbounded mediums with spherical cavities [37–44].

In the current article, magneto-thermoelastic exchanges in an infinite solid with a spherical hole are studied with respect to multi-time-derivative thermoelasticity theories [45–53]. A refined DPL model is used for this purpose. The technique of Laplace transforms in the time domain is applied to obtain the governing equations analytically. The derived equations are solved and then Laplace inversion is carried out to obtain the field quantities numerically. For verification proposes, the outcomes are compared with those obtained previously. Additional results are presented graphically and others are reported for future comparison.

2. Basic Equations

Let us be concerned with thermoelastic analysis of an isotropic body including a spherical cavity of radius R based on unified multi-phase-lag theory. It is assumed that the outer edge of the spherical cavity is traction-free and subjected to harmonically varying heat (See Figure 1). The spherical cavity coordinate system (r, θ, ϕ) is used to address the present problem.

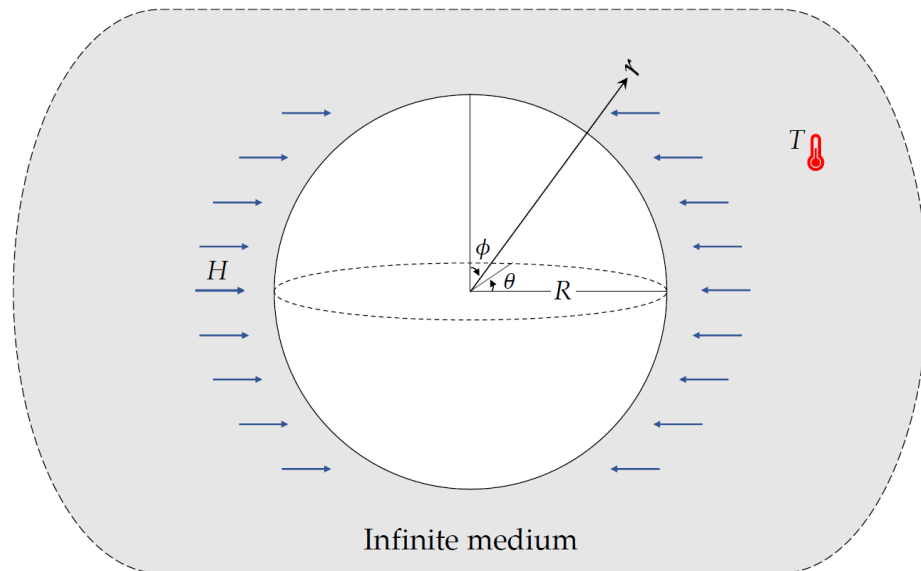


Figure 1. A spherical cavity in an unbounded medium under harmonically varying heat and external magnetic field.

The governing equations for a linear isotropic homogeneous thermoelastic body in the absence of volume forces are given by:

- The equations of motion:

$$\mu u_{i,jj} + (\lambda + \mu)u_{j,ij} - \gamma\Theta_{,i} = \rho \frac{\partial^2 u_i}{\partial t^2} \tag{1}$$

- The constitutive equations:

$$\sigma_{ij} = 2\mu e_{ij} + (\lambda e_{k,k} - \gamma\Theta)\delta_{ij} \tag{2}$$

where σ_{ij} and e_{ij} are the stresses and strains and δ_{ij} denotes Kronecker’s delta tensor.

- The heat conduction equation:

$$kL_T(\nabla^2\Theta) = L_q\left(\rho C_e \frac{\partial \Theta}{\partial t} + \gamma T_0 \frac{\partial u_{k,k}}{\partial t} - Q\right) \tag{3}$$

is considered in the context of the refined thermoelasticity form in which L_T and L_q denote the following higher-order time-derivative operators:

$$L_T = 1 + \sum_{n=1}^N \frac{\tau_T^n}{n!} \frac{\partial^n}{\partial t^n}, \quad L_q = \varrho + \sum_{n=1}^N \frac{\tau_q^n}{n!} \frac{\partial^n}{\partial t^n} \tag{4}$$

Equation (3) with the aid of Equation (2) are the more general ones when N has numerous integers more than zero. Some specific cases may be achieved as

- (i) Dynamical coupled thermoelasticity (CTE) model [4]: $\tau_T = \tau_q = 0$ and $\varrho = 1$,

$$k\nabla^2\Theta = \rho C_e \frac{\partial\Theta}{\partial t} + \gamma T_0 \frac{\partial u_{k,k}}{\partial t} - Q \quad (5)$$

- (ii) Lord and Shulman (L-S) model [5]: $\tau_T = 0$, $\tau_q = \tau_0$ and $\varrho = 1$,

$$k\nabla^2\Theta = \left(1 + \tau_q \frac{\partial}{\partial t}\right) \left(\rho C_e \frac{\partial\Theta}{\partial t} + \gamma T_0 \frac{\partial u_{k,k}}{\partial t} - Q\right) \quad (6)$$

- (iii) Green and Naghdi (G-N) model without energy dissipation [12–14]: $\tau_T = 0$, $\tau_q = 1$, $k \rightarrow k^*$, $N = 1$ and $\varrho = 0$,

$$k^*\nabla^2\Theta = \frac{\partial}{\partial t} \left(\rho C_e \frac{\partial\Theta}{\partial t} + \gamma T_0 \frac{\partial u_{k,k}}{\partial t} - Q\right) \quad (7)$$

- (iv) The simple dual-phase-lag (SDPL) model [50–52]: $\tau_q \geq \tau_T > 0$, $\varrho = 1$ and $N = 1$,

$$k\left(1 + \tau_T \frac{\partial}{\partial t}\right)\nabla^2\Theta = \left(1 + \tau_q \frac{\partial}{\partial t}\right) \left(\rho C_e \frac{\partial\Theta}{\partial t} + \gamma T_0 \frac{\partial u_{k,k}}{\partial t} - Q\right) \quad (8)$$

- (v) The refined with dual-phase-lag (RDPL) model [50–52]: $N > 1$, $\tau_q \geq \tau_T > 0$, and $\varrho = 1$,

$$k\left(1 + \sum_{n=1}^N \frac{\tau_T^n}{n!} \frac{\partial^n}{\partial t^n}\right)\nabla^2\Theta = \left(1 + \sum_{n=1}^N \frac{\tau_q^n}{n!} \frac{\partial^n}{\partial t^n}\right) \left(\rho C_e \frac{\partial\Theta}{\partial t} + \gamma T_0 \frac{\partial u_{k,k}}{\partial t} - Q\right) \quad (9)$$

The displacements of the present, axially symmetric spherical medium are summarized as

$$u_r = u(r, t), \quad u_\theta = u_\phi = 0 \quad (10)$$

The non-vanishing strains and volumetric strain can be expressed as

$$e_{rr} = \frac{\partial u}{\partial r}, \quad e_{\theta\theta} = e_{\phi\phi} = \frac{u}{r} \quad (11)$$

Thus, the volumetric strain e has the form

$$e = e_{rr} + e_{\theta\theta} + e_{\phi\phi} = \frac{\partial u}{\partial r} + \frac{2u}{r} = \frac{1}{r^2} \frac{\partial}{\partial r} (r^2 u) \quad (12)$$

The constitutive equations for the spherical symmetric system can be stated as

$$\sigma_{rr} = 2\mu \frac{\partial u}{\partial r} + \lambda e - \gamma\Theta \quad (13)$$

$$\sigma_{\theta\theta} = \sigma_{\phi\phi} = 2\mu \frac{u}{r} + \lambda e - \gamma\Theta \quad (14)$$

$$\left(2\mu + \lambda + \mu_0 H_0^2\right) \frac{\partial e}{\partial r} - \gamma \frac{\partial\Theta}{\partial r} = \rho \frac{\partial^2 u}{\partial t^2} \quad (15)$$

Applying the operator $(\partial/\partial r + 2/r)$ to both sides of Equation (15), one gets

$$\left(2\mu + \lambda + \mu_0 H_0^2\right) \nabla^2 e - \gamma \nabla^2 \Theta = \rho \frac{\partial^2 e}{\partial t^2} \quad (16)$$

in which ∇^2 denotes the Laplacian operator in spherical coordinates. It meets the formulation

$$\nabla^2(*) = \frac{\partial^2(*)}{\partial r^2} + \frac{2}{r} \frac{\partial(*)}{\partial r} = \frac{1}{r^2} \frac{\partial}{\partial r} \left(r^2 \frac{\partial(*)}{\partial r}\right) \quad (17)$$

3. Formulation of the Problem

It is proper to establish the non-dimensional variables in the following parts:

$$\begin{aligned} \{r', u'\} &= c_0 \eta \{r, u\}, \quad \{t', \tau'_T, \tau'_q\} = \eta c_0^2 \{t, \tau_T, \tau_q\}, \\ \sigma'_{ii} &= \frac{\sigma_{ii}}{\lambda + 2\mu}, \quad \Theta' = \frac{\gamma \Theta}{\lambda + 2\mu}, \quad c_0^2 = \frac{\lambda + 2\mu}{\rho}, \quad \eta = \frac{\rho C_e}{k} \end{aligned} \quad (18)$$

The whole governing equations, with the above dimensionless variables, are diminished to (throwing down the dash for convenience)

$$\sigma_{rr} = e - \frac{2}{c_1} \frac{u}{r} - \Theta \quad (19)$$

$$\sigma_{\theta\theta} = \sigma_{\phi\phi} = \left(1 - \frac{1}{c_1}\right) e + \frac{1}{c_1} \frac{u}{r} - \Theta \quad (20)$$

$$c_2 \nabla^2 e - \nabla^2 \Theta = \frac{\partial^2 e}{\partial t^2} \quad (21)$$

$$\left(\nabla^2 L_T - L_q \frac{\partial}{\partial t}\right) \Theta - \varepsilon L_q \left(\frac{\partial e}{\partial t}\right) = 0 \quad (22)$$

where

$$c_1 = \frac{\lambda + 2\mu}{2\mu}, \quad c_2 = 1 + \frac{\mu_0 H_0^2}{\lambda + 2\mu}, \quad \varepsilon = \frac{\gamma^2 T_0}{\rho C_e (\lambda + 2\mu)} \quad (23)$$

4. Closed-Form Solution

The comprehensive solutions are provided by resolving Equations (21) and (22) to obtain, firstly, temperature Θ and volumetric strain (dilatation) e . Then, the subsequent radial displacement and thermal stresses may be presented as functions of Θ and e . For this objective, we will first employ the next initial conditions:

$$u(r, 0) = \frac{\partial u}{\partial t} \Big|_{t=0} = 0, \quad \Theta(r, 0) = \frac{\partial \Theta}{\partial t} \Big|_{t=0} = 0, \quad R \leq r < \infty \quad (24)$$

In adding together to the above homogenous initial conditions, we also used the thermomechanical boundary conditions. The current unbounded body will be studied as quiescent and the surface of the spherical cavity is assumed to be exposed to constant heat and traction free. Such conditions can be explained as

- The surface of the spherical hole is subjected to a constant heat

$$\Theta(R, t) = \Theta_0 H(t), \quad t > 0 \quad (25)$$

- The mechanical boundary condition is respected as the surface of the spherical hole is traction free

$$\sigma_{rr}(R, t) = 0, \quad t > 0 \quad (26)$$

Moreover, we take into consideration the following regularity conditions

$$u(r, t) = 0, \quad \Theta(r, t) = 0, \quad r \rightarrow \infty \quad (27)$$

The Laplace transform is carried out for Equations (19)–(22), and, with the homogenous initial conditions that appeared in Equation (24), one gets:

$$\bar{\sigma}_{rr} = \bar{e} - \frac{2}{c_1} \frac{\bar{u}}{r} - \bar{\Theta} \quad (28)$$

$$\bar{\sigma}_{\theta\theta} = \bar{\sigma}_{\phi\phi} = \left(1 - \frac{1}{c_1}\right)\bar{e} + \frac{1}{c_1}\frac{\bar{u}}{r} - \bar{\Theta} \quad (29)$$

$$(c_2\nabla^2 - s^2)\bar{e} - \nabla^2\bar{\Theta} = 0 \quad (30)$$

$$(\nabla^2 - \omega)\bar{\Theta} - \varepsilon\omega\bar{e} = 0 \quad (31)$$

where

$$\omega = \frac{s\bar{L}_q}{\bar{L}_T}, \quad \bar{L}_T = 1 + \sum_{n=1}^N \frac{\tau_T^n}{n!} s^n, \quad \bar{L}_q = \varrho + \sum_{n=1}^N \frac{\tau_q^n}{n!} s^n \quad (32)$$

The system of equations provided in Equations (30) and (31) can be indicated in the differential equation

$$(\nabla^4 - \beta_1\nabla^2 + \beta_0)\bar{e}(r) = 0 \quad (33)$$

where the coefficients β_i are given by

$$\beta_0 = \frac{s^2\omega}{c_2}, \quad \beta_1 = \frac{s^2 + \omega(\varepsilon + c_2)}{c_2} \quad (34)$$

and the temperature $\bar{\Theta}$ is reformed as follows

$$\bar{\Theta}(r) = \frac{c_2}{\omega}\nabla^2\bar{e}(r) - \left(\frac{s^2}{\omega} + \varepsilon\right)\bar{e}(r) \quad (35)$$

Equation (33) is very complicated since it is presented in a polar coordinate system. It can be expressed as

$$(\nabla^2 - \zeta_1^2)(\nabla^2 - \zeta_2^2)\bar{e}(r) = 0 \quad (36)$$

where ζ_j^2 are the roots of

$$\zeta^4 - \beta_1\zeta^2 + \beta_0 = 0 \quad (37)$$

These roots ζ_j are given, respectively, by

$$\zeta_{1,2}^2 = \frac{1}{2}\left(\beta_1 \pm \sqrt{\beta_1^2 - 4\beta_0}\right) \quad (38)$$

Equation (36) tends to the next modified Bessel's equation of zero-order

$$\left(\frac{1}{r}\frac{\partial}{\partial r}\left(r\frac{\partial}{\partial r}\right) - \zeta_1^2\right)\left(\frac{1}{r}\frac{\partial}{\partial r}\left(r\frac{\partial}{\partial r}\right) - \zeta_2^2\right)\bar{e}(r) = 0 \quad (39)$$

which has a solution under the regularity conditions: $\bar{u}, \bar{\Theta} \rightarrow 0$ as $r \rightarrow \infty$. Therefore, the general solution of Equations (35) and (39), that is bounded at infinity, is provided by

$$\{\bar{\Theta}(r), \bar{e}(r)\} = \frac{1}{r} \sum_{j=1}^2 \{1, \zeta_j\} B_j e^{-\zeta_j r} \quad (40)$$

where B_j are integration parameters and

$$\zeta_j = \frac{c_2\bar{\zeta}_2^2 - s^2}{\omega} - \varepsilon \quad (41)$$

Using the relation between \bar{u} and \bar{e}

$$\bar{e}(r) = \mathcal{D}\bar{u}(r), \quad \mathcal{D} = \frac{d}{dr} + \frac{2}{r} \quad (42)$$

one can pick up the solution for the dimensionless form of radial displacement pretending that \bar{u} disappears at infinity as:

$$\bar{u}(r) = \sum_{j=1}^2 (1 - \hat{\zeta}_j) B_j e^{-\hat{\zeta}_j r} \quad (43)$$

where

$$\hat{\zeta}_j = 1 + \frac{1}{\zeta_j r} + \frac{1}{\zeta_j^2 r^2} \quad (44)$$

Up to here, the solution is finished. It is as much as needed to establish the two parameters B_j with the aid of the boundary conditions given in Equations (25) and (26). So, one gets

$$\bar{\sigma}_1 = \bar{\sigma}_{rr} = \frac{1}{r} \sum_{j=1}^2 \left[1 - \zeta_j + \frac{2}{c_1} (\hat{\zeta}_j - 1) \right] B_j e^{-\zeta_j r} \quad (45)$$

$$\bar{\sigma}_2 = \bar{\sigma}_{\theta\theta} = \bar{\sigma}_{\phi\phi} = \frac{1}{r} \sum_{j=1}^2 \left(1 - \frac{\hat{\zeta}_j}{c_1} - \zeta_j \right) B_j e^{-\zeta_j r} \quad (46)$$

Therefore, the current analytical solution is already provided for the modified formulations in Laplace space. To achieve the solution in the basic time-space one can consider a function $\psi(t)$ as an inversion of the Laplace function $\bar{\psi}(s)$ in the form

$$\psi(t) = \frac{e^{pt}}{t} \left[\frac{1}{2} \bar{\psi}(p) + \operatorname{Re} \left(\sum_{i=1}^L (-1)^i \bar{\psi} \left(p + \frac{i\pi}{t} \right) \right) \right] \quad (47)$$

where p is an arbitrary constant, Re is the real part, i suggests the imagined number unit and L denotes a sufficiently big integer. For faster combination, various numerical analyses have shown that the approximation of p fulfills the connection $pt \approx 4.7$ [35]. The numerical procedure cited is used to invert the terms of temperature Θ , radial displacement u , volumetric strain e , radial stress σ_1 , and circumferential stress σ_2 .

5. Validation

Numerous examples are presented to illustrate the effect of several models on the field variables. The material properties of the infinite medium with a spherical cavity are

$$\begin{aligned} \lambda &= 7.76 \times 10^{10} \text{ N m}^{-2}, \quad \mu = 3.86 \times 10^{10} \text{ N m}^{-2}, \quad C_e = 383.1 \text{ J kg}^{-1} \text{ K}^{-1}, \\ \alpha_t &= 1.78 \times 10^{-5} \text{ K}^{-1}, \quad \rho = 8954 \text{ kg m}^{-3}, \\ k &= 386 \text{ W m}^{-1} \text{ K}^{-1}, \quad T_0 = 293 \text{ K}, \quad k^* = 1.2 \end{aligned}$$

Numerical outcomes are attained (except where otherwise indicated) for $\Theta_0 = 10$, $\tau_q = 0.02$, $\tau_T = 0.018$, $t = 0.03$, and radius $R = 1$.

5.1. First Justification

The outcomes for all variables using various thermoelasticity models of dual-phase-lag are presented in Tables 1–5 at different positions. The impact of magnetic field μ_0 and H_0 on all field quantities of the various models are produced at dimensionless time $t = 0.03$. Additional results are illustrated in Figures 2–11 through the radial direction of an unbounded medium with a spherical hole.

Table 1. Effects of dimensionless time t on volumetric strain $\bar{\epsilon}$ according to different thermoelasticity theories with several values of r .

r	t	CTE	G–N	L–S	SDPL		RDPL	
					$N = 1$	$N = 3$	$N = 4$	$N = 5$
1.001	0.02	23.809257	3.0601024	24.0856	23.808792	23.808531	23.808844	23.809054
	0.03	21.299459	16.83015	21.555949	21.29979	21.30039	21.299517	21.295514
	0.05	16.62998	24.126713	16.819316	16.631298	16.631497	16.630909	16.636946
1.0108	0.02	9.048562	−0.1153723	8.8444984	9.0436695	9.0430854	9.0508697	9.0662687
	0.03	5.9635525	7.3662102	5.6387135	5.9605812	5.9665798	5.9730733	5.9683018
	0.05	9.6360547	7.6797451	9.459863	9.6357821	9.6349646	9.6210413	9.6310639
1.035	0.02	−0.1538211	−0.2026603	−0.4084073	−0.1628925	−0.1754834	−0.1766143	−0.1722681
	0.03	−0.2531288	−0.2064843	−0.2693186	−0.2655987	−0.2744405	−0.2676814	−0.2565349
	0.05	10.563634	−0.3048223	10.574561	10.558	10.573683	10.573157	10.549094

Table 2. Effects of dimensionless time t on radial displacement \bar{u} according to different thermoelasticity theories with several values of r .

r	t	CTE	G–N	L–S	SDPL		RDPL	
					$N = 1$	$N = 3$	$N = 4$	$N = 5$
1.02	0.02	0.016967	6.59×10^{-3}	0.02626	0.017492	0.018306	0.018521	0.018544
	0.03	−0.06242	0.012333	−0.05158	−0.06156	−0.06069	−0.06086	−0.06142
	0.05	−0.21674	0.023884	−0.20169	−0.21541	−0.21513	−0.21532	−0.2143
1.2	0.02	2.17×10^{-3}	6.68×10^{-11}	3.38×10^{-6}	2.04×10^{-3}	1.82×10^{-3}	1.73×10^{-3}	1.68×10^{-3}
	0.03	6.32×10^{-3}	5.89×10^{-7}	9.67×10^{-4}	6.12×10^{-3}	5.89×10^{-3}	5.91×10^{-3}	6.05×10^{-3}
	0.05	0.02141	1.46×10^{-6}	0.018332	0.021199	0.021304	0.021448	0.021156
1.4	0.02	1.09×10^{-4}	8.19×10^{-19}	7.92×10^{-8}	8.52×10^{-5}	5.03×10^{-5}	3.80×10^{-5}	2.83×10^{-5}
	0.03	6.20×10^{-4}	3.73×10^{-12}	1.20×10^{-6}	5.33×10^{-4}	4.03×10^{-4}	3.58×10^{-4}	3.26×10^{-4}
	0.05	3.81×10^{-3}	4.67×10^{-8}	8.92×10^{-6}	3.54×10^{-3}	3.30×10^{-3}	3.34×10^{-3}	3.47×10^{-3}

Table 3. Effects of dimensionless time t on temperature $\bar{\Theta}$ according to different thermoelasticity theories with several values of r .

r	t	CTE	G–N	L–S	SDPL		RDPL	
					$N = 1$	$N = 3$	$N = 4$	$N = 5$
1.02	0.02	12.4075	0.765094	2.199177	12.55818	12.92892	13.1502	13.34968
	0.03	11.96567	1.840952	14.22474	12.14601	12.5459	12.66462	12.52622
	0.05	11.31646	0.063337	22.12826	11.50767	11.8686	12.0525	12.76183
1.2	0.02	2.604722	-2.25×10^{-8}	0.014782	2.510894	2.453168	2.515533	2.661198
	0.03	3.361241	1.08×10^{-4}	4.068197	3.310861	3.477755	3.716377	4.020897
	0.05	4.423428	-1.49×10^{-4}	4.010311	4.357168	4.381843	4.120538	3.461431
1.4	0.02	0.325147	1.79×10^{-16}	1.45×10^{-4}	0.268041	0.181612	0.14935	0.122447
	0.03	0.733066	5.64×10^{-9}	4.00×10^{-4}	0.660726	0.580455	0.574048	0.591092
	0.05	1.471241	5.49×10^{-5}	0.06287	1.423396	1.488998	1.566341	1.558591

Table 4. Effects of dimensionless time t on radial stress $\bar{\sigma}_1$ according to different thermoelasticity theories with several values of r .

r	t	CTE	G–N	L–S	SDPL		RDPL	
					$N = 1$	$N = 3$	$N = 4$	$N = 5$
1.02	0.02	−8.18367	−0.89255	2.057934	−8.34605	−8.73216	−8.95355	−9.14535
	0.03	−1.07491	−2.14559	−3.37834	−1.26233	−1.65585	−1.75897	−1.60453
	0.05	−4.01791	−0.38448	−15.1083	−4.2121	−4.56849	−4.77181	−5.5112
1.2	0.02	−2.6318	2.61×10^{-8}	−0.01511	−2.53776	−2.47972	−2.54218	−2.68827
	0.03	−3.42287	$−1.26 \times 10^{-4}$	−4.15875	−3.37323	−3.54214	−3.78243	−4.08913
	0.05	−4.57844	1.71×10^{-4}	−4.20834	−4.51548	−4.54388	−4.28088	−3.61623
1.4	0.02	−0.32688	$−2.07 \times 10^{-15}$	$−1.48 \times 10^{-4}$	−0.2695	−0.1826	−0.15016	−0.1231
	0.03	−0.74048	$−6.54 \times 10^{-9}$	$−4.15 \times 10^{-4}$	−0.6675	−0.58625	−0.57954	−0.59643
	0.05	−1.50361	$−6.36 \times 10^{-5}$	0.064107	−1.45493	−1.52053	−1.59878	−1.59192

Table 5. Effects of dimensionless time t on circumferential stress $\bar{\sigma}_2$ according to different thermoelasticity theories with several values of r .

r	t	CTE	G–N	L–S	SDPL		RDPL	
					$N = 1$	$N = 3$	$N = 4$	$N = 5$
1.02	0.02	−10.2735	−0.82254	−0.03941	−10.4295	−10.8072	−11.0283	−11.2239
	0.03	−6.56734	−1.98159	−8.83803	−6.75038	−7.14623	−7.2573	−7.1114
	0.05	−7.86997	−0.20094	−18.8067	−8.06137	−8.41975	−8.61358	−9.33697
1.2	0.02	−2.61649	2.44×10^{-8}	−0.01494	−2.52266	−2.46497	−2.52745	−2.67337
	0.03	−3.38687	$−1.17 \times 10^{-4}$	−4.11278	−3.33703	−3.50513	−3.74457	−4.05007
	0.05	−4.48332	1.61×10^{-4}	−4.09433	−4.41888	−4.44534	−4.18307	−3.52142
1.4	0.02	−0.32594	$−1.93 \times 10^{-15}$	$−1.46 \times 10^{-4}$	−0.26871	−0.18207	−0.14973	−0.12275
	0.03	−0.73634	$−6.09 \times 10^{-9}$	$−4.07 \times 10^{-4}$	−0.66374	−0.58307	−0.57655	−0.59354
	0.05	−1.48475	$−5.92 \times 10^{-5}$	0.063495	−1.43668	−1.50245	−1.58022	−1.57282

The outcomes described in Tables 1–5 are offered as benchmarks for other researchers. It is evident from the tabulated results that:

- The G–N model provides the lowest absolute value of all variables. It may vanish at some positions.
- The other CTE and L–S models provide appropriate outcomes for all variables.
- Triplet values $N = 3, 4,$ and 5 are utilized for the RDPL model while the SDPL model is defined with $N = 1$.
- Extremely exact outcomes are provided utilizing the RDPL model.
- For the RDPL model the temperature, displacement, and circumferential stress slightly increase as the value of N increases, while volumetric strain, radial stress, and circumferential stress slightly decrease. All variables may be insensitive to the higher values of N especially when $N \geq 5$.

5.2. Second Justification

Figures 2–6 show the effect of all models on the variables with fixed time $t = 0.03$. The remainder of the graphs are exhibited in relation to the refined dual-phase-lag (RDPL) model with $N = 5$ to examine the effect of various parameters on all field variables.

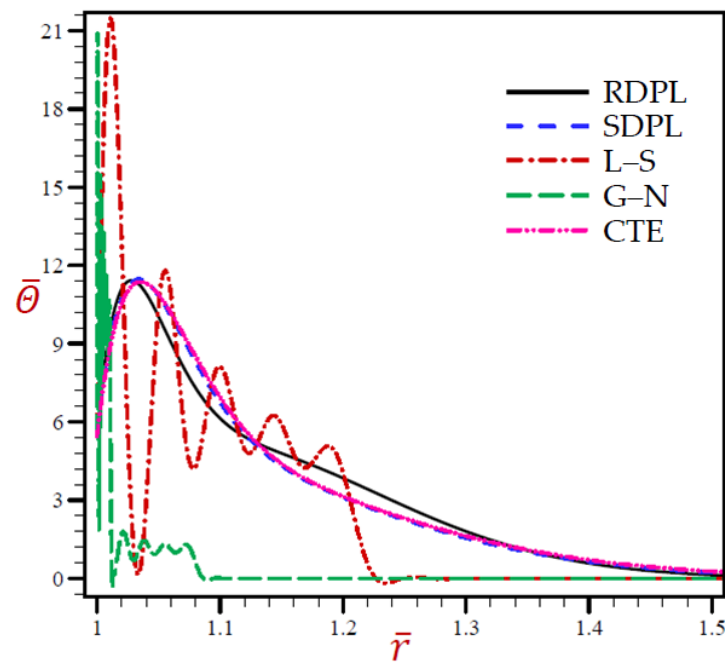


Figure 2. The temperature $\bar{\theta}$ through radial direction of spherical hole presenting to all models.

The discrepancy of the temperature $\bar{\theta}$ through radial direction of a spherical hole corresponding to all models is produced in Figure 2. Similar figures for the remaining variables are presented in Figures 3–6. Figure 2 reveals that the temperature due to the CTE, L-S, and SDPL models vibrates across the trajectory of the RDPL model, while temperature due to the G–N model vibrates below the trajectory of the RDPL model. The temperature according to the G–N model may vanish earlier than the temperature according to other models.

Figure 3 reveals that the values of \bar{e} of SDPL, L-S, and CTE models vibrate identically to the trajectory of the RDPL theory. While the value of \bar{e} for the G–N model vibrates across and below the trajectory of the RDPL model.

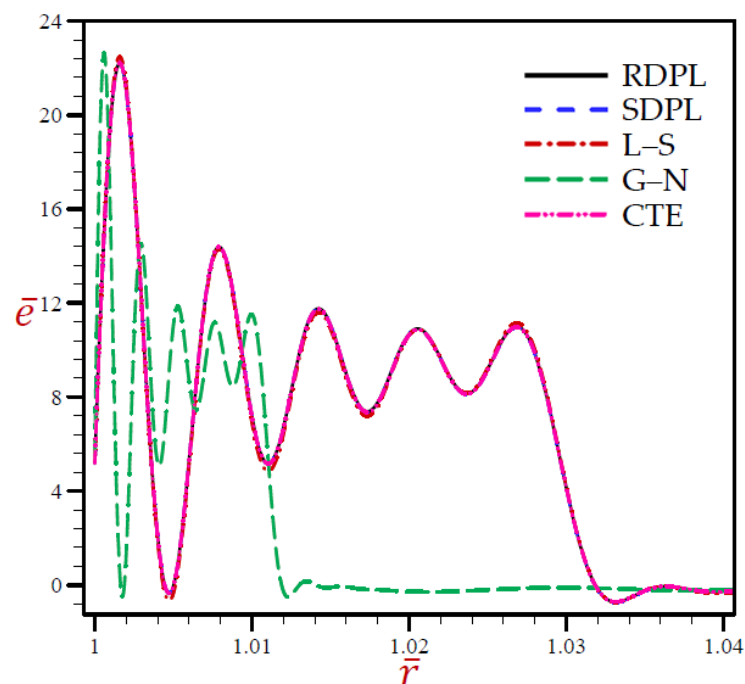


Figure 3. The volumetric strain \bar{e} through radial direction of a spherical hole presenting to all models.

Figure 4 indicates that the radial displacements \bar{u} of the CTE and SDPL models may be the same as those of RDPL theory, vanishing through radial direction. The displacements \bar{u} of the L–S model may be the upper or lower bounds of those due to the RDPL model. The G–N model always produces the smallest displacement during the radial direction.

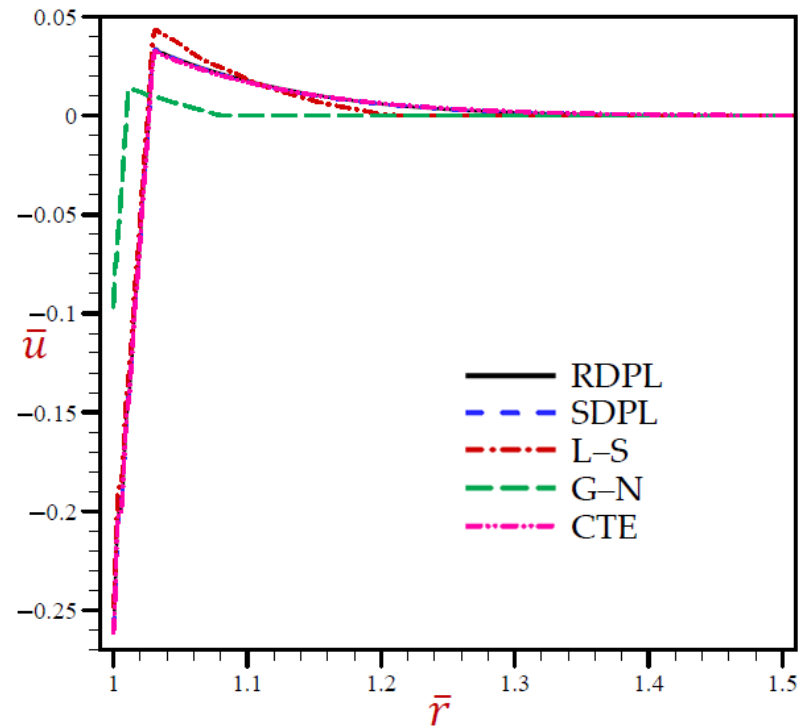


Figure 4. The radial displacement \bar{u} through radial direction of spherical hole presenting to all models.

Figure 5 reveals that the radial stress $\bar{\sigma}_1$ of the G–N model may rapidly vanish through the radial direction when $r > 1.1$. The radial stress of the L–S model vibrates around the RDPL model with wide amplitude, then it also vanishes when $r > 1.24$. The other CTE and SDPL theories give radial stresses that vibrate around those of the RDPL theory but with small amplitude.

Finally, Figure 6 shows similar behaviors of circumferential stress as those of the radial stress. It shows that the circumferential stress $\bar{\sigma}_2$ of the G–N model may rapidly vanish through the radial direction when $r > 1.1$. The radial stress of the L–S model vibrates around the RDPL theory with wide amplitude, then it also vanishes when $r > 1.24$. The other CTE and SDPL theories give radial stresses that vibrate around those of the RDPL theory but with small amplitude.

It is concluded from the above figures that the outcomes of the RDPL model are the most straightforward. So, we restrict our attention to using this theory for yielding the outcomes of this problem considering the effect of various parameters on the field variables.

5.3. The Influence of Dimensionless Time

The outcomes of dimensionless time t on all variables due to the RDPL model are presented in Figures 7–11. Figure 7 reveals the effects of t on $\bar{\Theta}$ through radial direction of a spherical hole. Similar figures for the remaining variables are presented in Figures 8–11. It is clear in Figure 7 that $\bar{\Theta}$ vibrates through the radial direction for various values of t with different wavelengths. The temperature $\bar{\Theta}$ no longer increases and has its highest values when $r = 1.04$. The temperature vanishes as r increases, irrespective of the values of t .

Figure 8 reveals that the volumetric strain $\bar{\epsilon}$ vibrates through the radial direction of a spherical hole with different amplitudes and different wavelengths. The wavelength increases as t increases. For $t = 0.02$ the volumetric strain $\bar{\epsilon}$ firstly vanishes when $r > 1.024$,

while for $t = 0.05$, the volumetric strain $\bar{\epsilon}$ finally vanishes when $r > 1.06$. In Figure 9, the radial displacement \bar{u} rapidly increases through the radial direction of the spherical hole when $t = 0.02$, while \bar{u} slowly increases when $t = 0.03$. \bar{u} is slowly decreasing when $t = 0.05$. It is obvious that the radial displacement \bar{u} increases with increase in dimensionless time t at fixed positions.

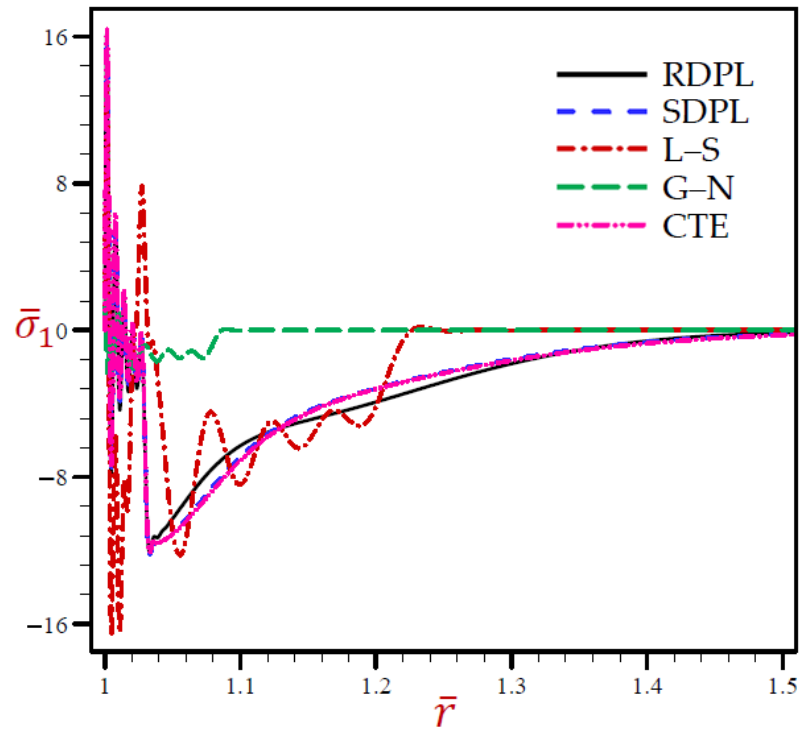


Figure 5. The radial stress $\bar{\sigma}_1$ through radial direction of spherical hole presenting to all models.

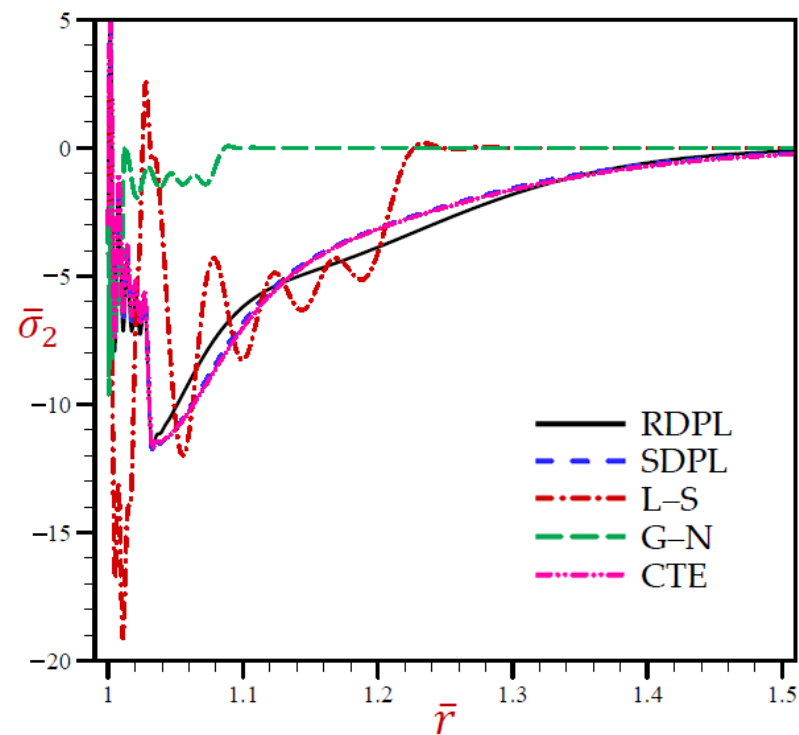


Figure 6. The circumferential stress $\bar{\sigma}_2$ through radial direction of a spherical hole presenting to all models.

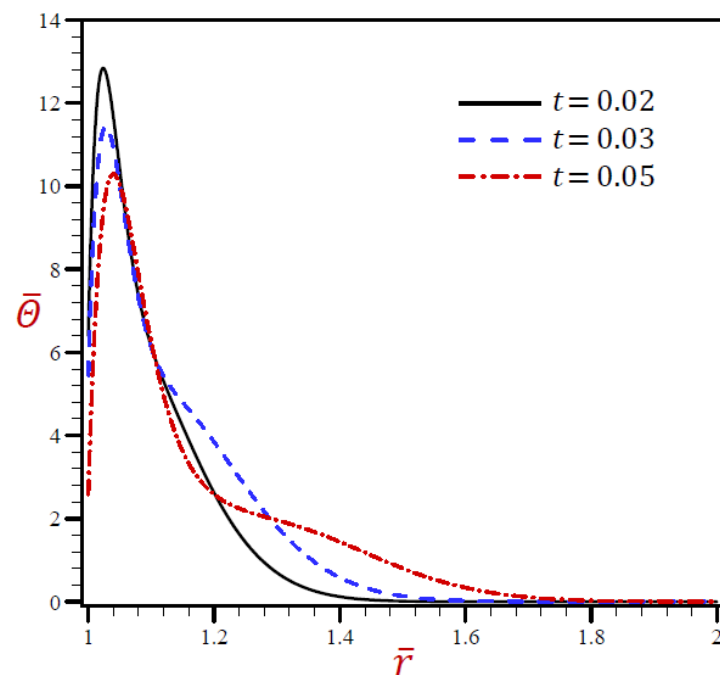


Figure 7. The influence of t on temperature $\bar{\Theta}$ through radial direction of a spherical hole using RDPL model.

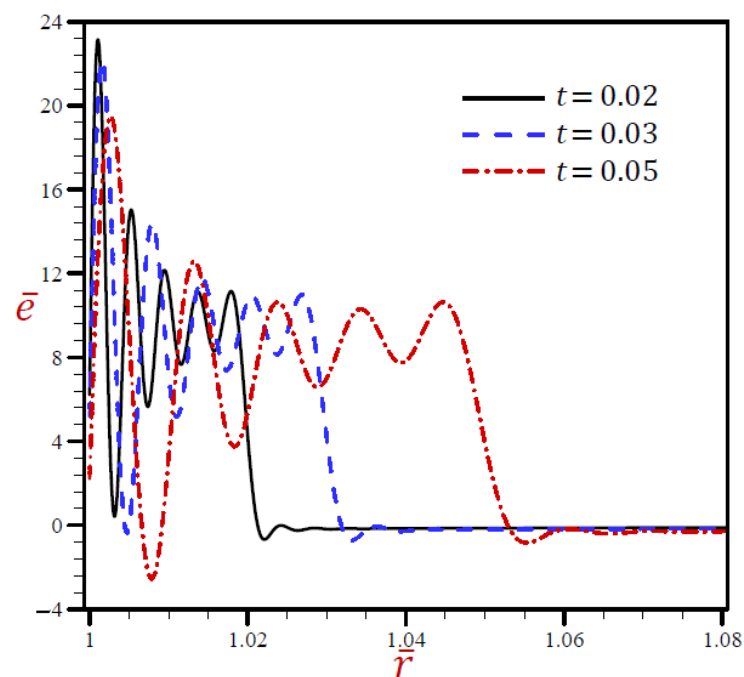


Figure 8. The influence of t on volumetric strain \bar{e} through radial direction of spherical hole using RDPL model.

The radial stress $\bar{\sigma}_1$ through the radial direction of spherical hole due to the RDPL model is described in Figure 10 for various values of t . The radial stress $\bar{\sigma}_1$ oscillates on a very small scale, then increases when $t = 0.03$ and 0.05 , while it decreases when $t = 0.02$. At any fixed position, the radial stress $\bar{\sigma}_1$ increases with increase in the dimensionless time t . The circumferential stress $\bar{\sigma}_2$ is drawn through the radial direction of the spherical cavity utilizing the RDPL model in Figure 11 for distinctive values of t . It vibrates over a very small range, then it increases for $t = 0.02$, but decreases when $t = 0.03$ and 0.05 . At any

fixed position, the circumferential stress $\bar{\sigma}_2$ increases with increase in the dimensionless time t .

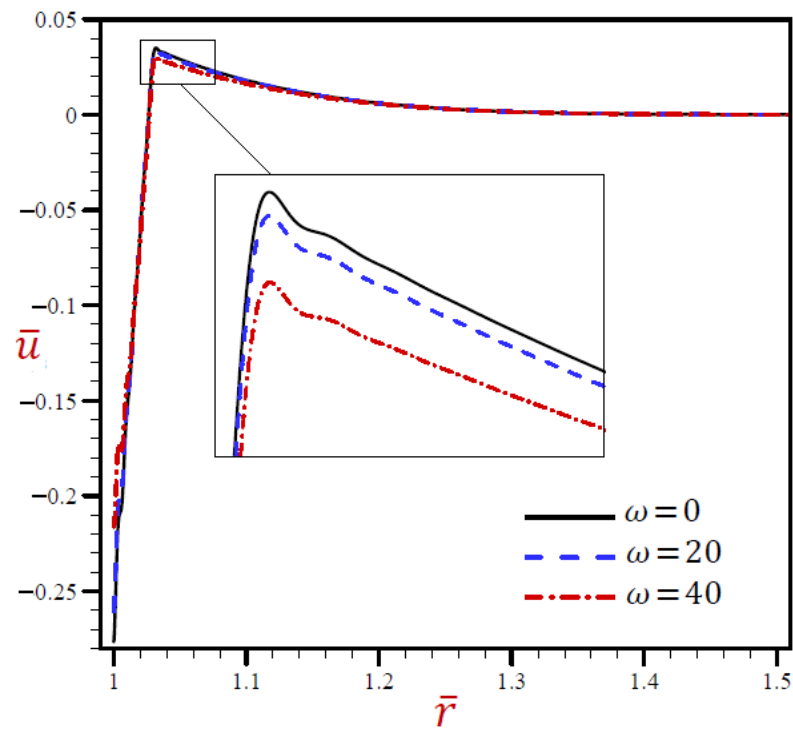


Figure 9. The influence of t on radial displacement \bar{u} through radial direction of spherical hole using RDPL model.

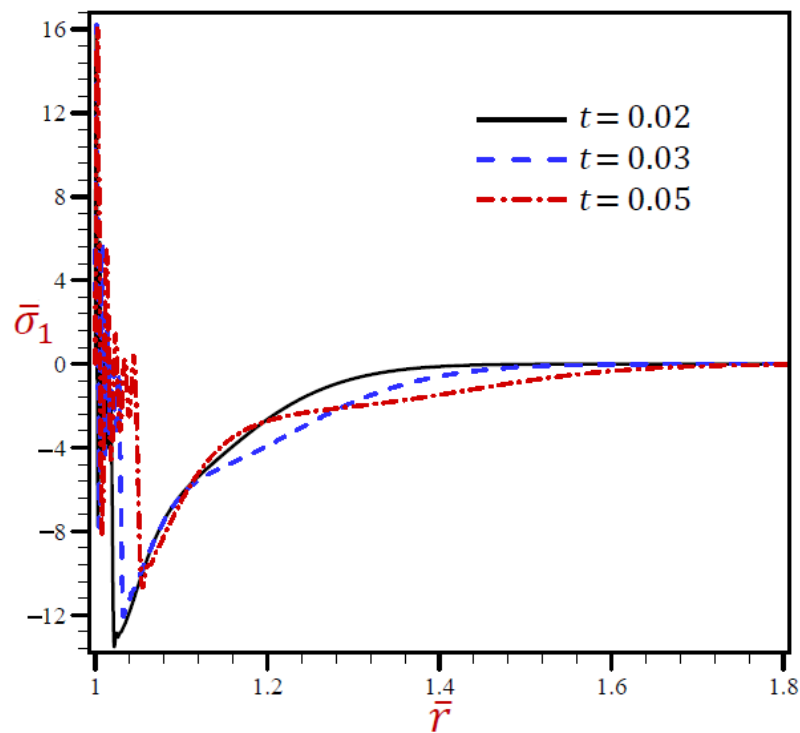


Figure 10. The influence of t on radial stress $\bar{\sigma}_1$ through radial direction of spherical hole using RDPL model.

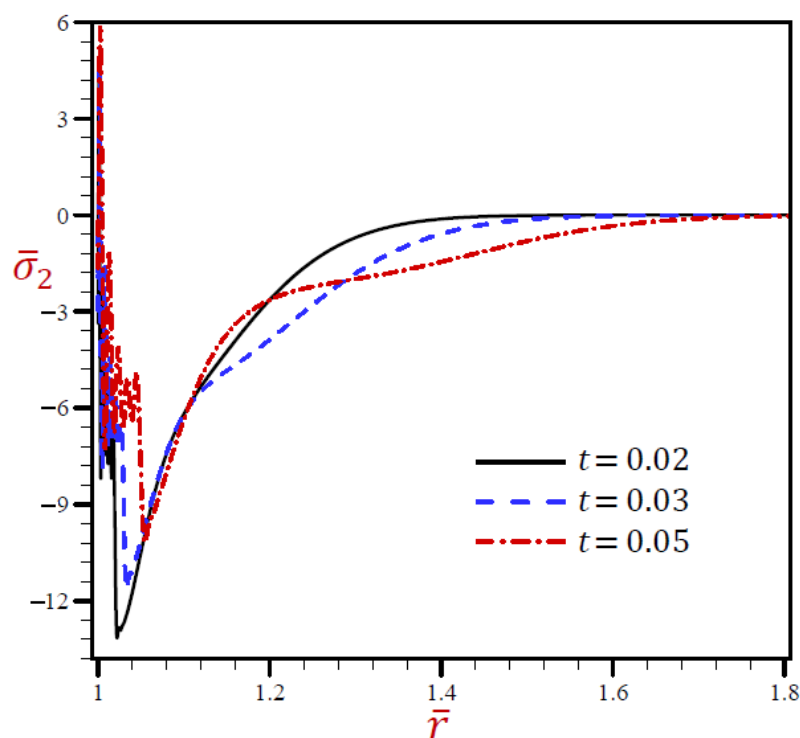


Figure 11. The influence of t on circumferential stress $\bar{\sigma}_2$ through radial direction of spherical hole using RDPL model.

6. Conclusions

The present refined dual-phase-lag model is innovative and produces accurate results for variables such as temperature, volumetric strain, displacement, and stresses. The multi-time derivatives heat equation was explained. The constitutive relations of spherical coordinates were considered to examine the thermoelastic coupling behavior of an infinite medium with a spherical cavity due to a uniform heat. To create a unified model, one can combine other models, including the coupled dynamical thermoelasticity model, the Lord and Shulman model, the Green and Naghdi model without energy dissipation, as well as a simple dual-phase-lag model. The system of two high-time-derivative differential coupled equations was solved, and all field variables were developed for the thermoelastic coupling response of an infinite medium with a spherical hole. Various confirmation examples and applications were offered to compare the outcomes due to all models with the refined ones. A sample set of graphs were presented to demonstrate relationships of variables through radial direction of a spherical hole. Some tables have been provided as confirmation examples to provide benchmark outcomes for future comparisons by other researchers. The described and demonstrated outcomes revealed different behaviors of all field variables and dimensionless time parameters. The present dual-phase-lag theory diminished the magnitudes of the examined variables, which may be significant in some practical applications. The G–N model provided appropriate outcomes over a small range. However, the refined model produced improved and exact outcomes.

Author Contributions: Conceptualization, A.M.Z., D.S.M. and A.M.A.; data collection, A.M.A.; methodology, A.M.Z. and A.M.A.; software, A.M.Z. and A.M.A.; validation, A.M.Z. and D.S.M.; writing—original draft preparation, D.S.M. and A.M.A.; writing—review and editing, A.M.Z. All authors have read and agreed to the published version of the manuscript.

Funding: This research received no external funding.

Institutional Review Board Statement: Not applicable.

Informed Consent Statement: Not applicable.

Data Availability Statement: Not applicable.

Conflicts of Interest: The authors declare no conflict of interest.

Nomenclature

α_t	thermal expansion (K^{-1})
C_θ	specific heat ($\text{J kg}^{-1} \text{K}^{-1}$)
δ_{ij}	Kronecker's delta
$e_{\theta\theta}, e_{\phi\phi}$	circumferential strains
e_{rr}	radial strain
e	volumetric strain (dilatation)
e_{ij}	strain tensor components
ϑ	velocity of heat source (m s^{-1})
$\gamma \equiv (3\lambda + 2\mu)\alpha_t$	thermal modulus ($\text{N m}^{-2} \text{K}^{-1}$)
$H(t)$	Heaviside's unit step function
H_0	initial magnetic field
k	heat conductivity ($\text{W m}^{-1} \text{K}^{-1}$)
k^*	rate of thermal conductivity ($\text{W m}^{-1} \text{K}^{-1}$)
λ, μ	Lame's constants (N m^{-2})
μ_0	electric permeability
ρ	density (kg m^{-3})
R	radius of the spherical hole (m)
(r, θ, ϕ)	spherical coordinates system
σ_{ij}	stress tensor components (N m^{-2})
$\sigma_{\theta\phi}, \sigma_{r\theta}, \sigma_{r\phi}$	shear stresses (N m^{-2})
$\sigma_{\theta\theta}, \sigma_{\phi\phi}$	circumferential stresses (N m^{-2})
σ_{rr}	radial stress (N m^{-2})
s	Laplace parameter
$\Theta = T - T_0$	temperature change (K)
Θ_0	thermal constant (K)
T_0	environment temperature (K)
τ_q	phase-lag of heat flux (s)
τ_T	phase-lag of temperature gradient (s)
τ_0	first relaxation time (s)
ω	angular frequency of thermal vibration (rad s^{-1})
Q_0	strength of heat source (W m^{-3})
δ	delta function
\vec{q}	heat flux vector (W m^{-2})
u_r	radial displacement (m)
u_θ, u_ϕ	circumferential displacements (m)

References

1. Maxwell, J. On the dynamical theory of gases. *J. Phil. Trans. Roy. Soc. Lond.* **1867**, *157*, 49–88.
2. Cattaneo, C. Sulla conduzione del calore. *Atti Del Semin. Matem. E Fis. Della Univ. Modena* **1948**, *3*, 83–101.
3. Dhaliwal, R.; Sherief, H. Generalized thermoelasticity for anisotropic media. *Quart. Appl. Math.* **1980**, *33*, 1–8. [[CrossRef](#)]
4. Biot, M.A. Thermoelasticity and irreversible thermodynamics. *J. Appl. Phys.* **1956**, *27*, 240–253. [[CrossRef](#)]
5. Lord, H.W.; Shulman, Y. A generalized dynamical theory of thermoelasticity. *J. Mech. Phys. Solids* **1967**, *15*, 299–309. [[CrossRef](#)]
6. Banerjee, S.; Roychoudhuri, S.K. Spherically symmetric thermo-visco-elastic waves in a visco-elastic medium with a spherical cavity. *Comput. Math. Appl.* **1995**, *30*, 91–98. [[CrossRef](#)]
7. Sinha, S.B.; Elsibai, K.A. Thermal stresses for an infinite body with spherical cavity with two relaxation times. *J. Therm. Stresses* **1996**, *19*, 495–510. [[CrossRef](#)]

8. Rakshit Kundu, M.; Mukhopadhyay, B. A thermoviscoelastic problem of an infinite medium with a spherical cavity using generalized theory of thermoelasticity. *Math. Comput. Model.* **2005**, *41*, 25–32. [[CrossRef](#)]
9. Youssef, H.M. Generalized thermoelastic infinite medium with spherical cavity subjected to moving heat source. *Comput. Math. Model.* **2010**, *21*, 212–225. [[CrossRef](#)]
10. Elhagary, M.A. Generalized thermoelastic diffusion problem for an infinite medium with a spherical cavity. *Int. J. Thermophys.* **2012**, *33*, 172–183. [[CrossRef](#)]
11. Karmakar, R.; Sur, A.; Kanoria, M. Generalized thermoelastic problem of an infinite body with a spherical cavity under dual-phase-lags. *J. Appl. Mech. Tech. Phys.* **2016**, *57*, 652–665. [[CrossRef](#)]
12. Green, A.E.; Naghdi, P.M. A re-examination of the basic postulates of thermomechanics. *Proc. R. Soc. A* **1991**, *432*, 171–194.
13. Green, A.E.; Naghdi, P.M. On undamped heat waves in an elastic solid. *J. Therm. Stresses* **1992**, *15*, 253–264. [[CrossRef](#)]
14. Green, A.E.; Naghdi, P.M. Thermoelasticity without energy dissipation. *J. Elast.* **1993**, *31*, 189–208. [[CrossRef](#)]
15. Mukhopadhyay, S. Thermoelastic interactions without energy dissipation in an unbounded medium with a spherical cavity due to a thermal shock at the boundary. *J. Therm. Stresses* **2002**, *25*, 877–887. [[CrossRef](#)]
16. Mukhopadhyay, S. Thermoelastic interactions without energy dissipation in an unbounded body with a spherical cavity subjected to harmonically varying temperature. *Mech. Res. Commun.* **2004**, *31*, 81–89. [[CrossRef](#)]
17. Mukhopadhyay, S.; Kumar, R. A study of generalized thermoelastic interactions in an unbounded medium with a spherical cavity. *Comput. Math. Appl.* **2008**, *56*, 2329–2339. [[CrossRef](#)]
18. Allam, M.N.; Elsibai, K.A.; Abouelregal, A.E. Magneto-thermoelasticity for an infinite body with a spherical cavity and variable material properties without energy dissipation. *Int. J. Solids Struct.* **2010**, *47*, 2631–2638. [[CrossRef](#)]
19. Banik, S.; Kanoria, M. Two-temperature generalized thermoelastic interactions in an infinite body with a spherical cavity. *Int. J. Thermophys.* **2011**, *32*, 1247–1270. [[CrossRef](#)]
20. Abbas, I.A. A GN model based upon two-temperature generalized thermoelastic theory in an unbounded medium with a spherical cavity. *Appl. Math. Comput.* **2014**, *245*, 108–115. [[CrossRef](#)]
21. Bera, M.B.; Das, N.C.; Lahiri, A. Thermoelastic wave with energy dissipation in an unbounded medium with a spherical cavity. *J. Therm. Stresses* **2014**, *37*, 1482–1494. [[CrossRef](#)]
22. Biswas, S. Thermoelastic interaction in unbounded transversely isotropic medium containing spherical cavity with energy dissipation. *Indian J. Phys.* **2021**, *95*, 705–716. [[CrossRef](#)]
23. Chandrasekharaiah, D.S.; Narasimha Murthy, H. Thermoelastic interactions in an unbounded body with a spherical cavity. *J. Therm. Stresses* **1993**, *16*, 55–70. [[CrossRef](#)]
24. Green, A.E.; Lindsay, K.A. Thermoelasticity. *J. Elast.* **1972**, *2*, 1–7. [[CrossRef](#)]
25. Roy Choudhuri, S.K.; Chatterjee, G. Spherically symmetric thermoelastic waves in a temperature-rate dependent medium with a spherical cavity. *Comput. Math. Appl.* **1990**, *20*, 1–12. [[CrossRef](#)]
26. Sherief, H.H.; Darwish, A.A. A short time solution for a problem in thermoelasticity of an infinite medium with a spherical cavity. *J. Therm. Stresses* **1998**, *21*, 811–828. [[CrossRef](#)]
27. Mukhopadhyay, S. Relaxation effects on thermally induced vibrations in a generalized thermoviscoelastic medium with a spherical cavity. *J. Therm. Stresses* **1999**, *22*, 829–840. [[CrossRef](#)]
28. Ghosh, M.K.; Kanoria, M. Generalized thermoelastic functionally graded spherically isotropic solid containing a spherical cavity under thermal shock. *Appl. Math. Mech.-Engl. Ed.* **2008**, *29*, 1263–1278. [[CrossRef](#)]
29. Kanoria, M.; Ghosh, M.K. Study of dynamic response in a functionally graded spherically isotropic hollow sphere with temperature dependent elastic parameters. *J. Therm. Stresses* **2010**, *33*, 459–484. [[CrossRef](#)]
30. Das, B.; Lahiri, A. A generalized thermoelastic problem of functionally graded spherical cavity. *J. Therm. Stresses* **2015**, *38*, 1183–1198. [[CrossRef](#)]
31. Tzou, D.Y. A unified approach for heat conduction from macro- to micro-scales. *J. Heat Transf.* **1995**, *117*, 8–16. [[CrossRef](#)]
32. Tzou, D.Y. *Macro- to Microscale Heat Transfer: The Lagging Behavior*, 2nd, ed.; Wiley: Hoboken, NJ, USA, 2015.
33. Abouelregal, A.E.; Abo-Dahab, S.M. Dual phase lag model on magneto-thermoelasticity infinite non-homogeneous solid having a spherical cavity. *J. Therm. Stresses* **2012**, *35*, 820–841. [[CrossRef](#)]
34. Hobiny, A.D.; Abbas, I.A. A DPL model of photo-thermal interaction in an infinite semiconductor material containing a spherical hole. *Eur. Phys. J. Plus* **2018**, *133*, 11. [[CrossRef](#)]
35. Mondal, S.; Sur, A. Photo-thermo-elastic wave propagation in an orthotropic semiconductor with a spherical cavity and memory responses. *Waves Random Complex Media* **2021**, *31*, 1835–1858. [[CrossRef](#)]
36. Singh, B.; Sarkar, S.P. State-space approach on two-temperature three-phase-lag thermoelastic medium with a spherical cavity due to memory-dependent derivative. *Arch. Appl. Mech.* **2021**, *91*, 3273–3290. [[CrossRef](#)]
37. Sherief, H.H.; Saleh, H.A. A problem for an infinite thermoelastic body with a spherical cavity. *Int. J. Eng. Sci.* **1998**, *36*, 473–487. [[CrossRef](#)]
38. Aouadi, M. A problem for an infinite elastic body with a spherical cavity in the theory of generalized thermoelastic diffusion. *Int. J. Solids Struct.* **2007**, *44*, 5711–5722. [[CrossRef](#)]
39. Banik, S.; Kanoria, M. Effects of three-phase-lag on two-temperature generalized thermoelasticity for infinite medium with spherical cavity. *Appl. Math. Mech.-Engl. Ed.* **2012**, *33*, 483–498. [[CrossRef](#)]

40. Abd-Alla, A.M.; Abo-Dahab, S.M. Effect of rotation and initial stress on an infinite generalized magneto-thermoelastic diffusion body with a spherical cavity. *J. Therm. Stresses* **2012**, *35*, 892–912. [[CrossRef](#)]
41. Lotfy, K. A novel solution of fractional order heat equation for photothermal waves in a semiconductor medium with a spherical cavity. *Chaos Solitons Fractals* **2017**, *99*, 233–242. [[CrossRef](#)]
42. Sherief, H.H.; Hussein, E.M. Contour integration solution for a thermoelastic problem of a spherical cavity. *Appl. Math. Comput.* **2018**, *320*, 557–571. [[CrossRef](#)]
43. Hendy, M.H.; Amin, M.M.; Ezzat, M.A. Magneto-electric interactions without energy dissipation for a fractional thermoelastic spherical cavity. *Microsys. Technol.* **2018**, *24*, 2895–2903. [[CrossRef](#)]
44. Sharma, D.K.; Bachher, M.; Sarkar, N. Effect of phase-lags on the transient waves in an axisymmetric functionally graded viscothermoelastic spherical cavity in radial direction. *Int. J. Dyn. Control* **2021**, *9*, 424–437. [[CrossRef](#)]
45. Zenkour, A.M. Thermo-diffusion of solid cylinders based upon refined dual-phase-lag models. *Multidiscip. Model. Mater. Struct.* **2020**, *16*, 1417–1434. [[CrossRef](#)]
46. Zenkour, A.M. Wave propagation of a gravitated piezo-thermoelastic half-space via a refined multi-phase-lags theory. *Mech. Adv. Mater. Struct.* **2020**, *27*, 1923–1934. [[CrossRef](#)]
47. Zenkour, A.M. Thermoelastic diffusion problem for a half-space due to a refined dual-phase-lag Green–Naghdi model. *J. Ocean Eng. Sci.* **2020**, *5*, 214–222. [[CrossRef](#)]
48. Zenkour, A.M. Thermal-shock problem for a hollow cylinder via a multi-dual-phase-lag theory. *J. Therm. Stresses* **2020**, *43*, 687–706. [[CrossRef](#)]
49. Zenkour, A.M. Exact coupled solution for photothermal semiconducting beams using a refined multi-phase-lag theory. *Opt. Laser Technol.* **2020**, *128*, 106233. [[CrossRef](#)]
50. Zenkour, A.M. Thermal diffusion of an unbounded solid with a spherical cavity via refined three-phase-lag Green–Naghdi models. *Indian J. Phys.* **2022**, *96*, 1087–1104. [[CrossRef](#)]
51. Kutbi, M.A.; Zenkour, A.M. Refined dual-phase-lag Green–Naghdi models for thermoelastic diffusion in an infinite medium. *Waves Random Complex Media* **2022**, *32*, 947–967. [[CrossRef](#)]
52. Zenkour, A.M.; El-Mekawy, H.F. On a multi-phase-lag model of coupled thermoelasticity. *Int. Commun. Heat Mass Transf.* **2020**, *116*, 104722. [[CrossRef](#)]
53. Sobhy, M.; Zenkour, A.M. Modified three-phase-lag Green–Naghdi models for thermomechanical waves in an axisymmetric annular disk. *J. Therm. Stresses* **2020**, *43*, 1017–1029. [[CrossRef](#)]